

Infrared Optical Absorption in Semiconducting CdF₂:Y Crystals

F. MOSER, D. MATZ, AND S. LYU

Research Laboratories, Eastman Kodak Company, Rochester, New York 14650

(Received 5 February 1969)

The infrared optical absorption band associated with yttrium (Y) donors in semiconducting CdF₂ has been measured over a broad range of donor concentration and temperature. The results are presented and discussed in terms of continuum theories for the electron energy states of isolated hydrogenlike centers in polar materials. The general features of the optical absorption are approximately described in terms of the nonadiabatic approximation, in which the lattice is polarized to a considerable extent by the instantaneous position of the electron. By assuming that the donors tend to form clusters, apparent discrepancies between the optical and transport properties can be resolved. Impurity-banding effects, which are extremely important in determining the transport properties, are relatively unimportant in interpreting the observed optical absorption.

I. INTRODUCTION

IN this paper we report the results of a systematic study of the infrared optical absorption in Y-doped semiconducting CdF₂ and discuss the observations in the context of available theories for trapped electron centers in polar materials.

Pure CdF₂ is a transparent, ionic solid at room temperature, with a resistivity of the order of 10⁷ Ω cm. It can be doped with a variety of trivalent cations, which enter the lattice substitutionally for Cd and are charge-compensated by interstitial fluoride ions.¹ Such doped crystals are generally still relatively insulating and optically transparent in the region from the band gap at about 6 eV to the reststrahl band in the infrared. In effect, millimeter-thick crystals have no measurable absorption in the spectral range from 6 to ~0.07 eV. When such crystals are heated in Cd metal vapor, the conductivity increases by many orders of magnitude, and an intense infrared optical absorption band appears. The conductivity and absorption are related to electrons injected into the crystal by the Cd annealing process. Interstitial fluoride ions equivalent in number to the injected electrons are removed in the same process. A number of studies of the optical and electrical properties of such crystals have been reported.²⁻⁵

The optical and electrical properties of electrons in CdF₂ are of course affected by the ionic character of the material. The static and high-frequency dielectric constants of CdF₂ are about 8 and 2.4, respectively.⁶ On the basis of transport studies of Y-doped crystals, Khosla and Matz⁷ (KM) deduce a polaron mass of about 0.9*m*_e, a bare conduction-band mass of 0.45*m*_e,

and a coupling constant of about 3.3 for electrons in CdF₂. Recently, Eisenberger *et al.*⁸ (EPB), on the basis of cyclotron resonance measurements, have reported a strikingly large polaron mass of about 11*m*_e and a coupling constant of about 6. This discrepancy has not been resolved. However, the transport measurements of KM were made on carriers in thermal equilibrium in the conduction band, while EPB measured the resonance of photoexcited carriers, which may not be in conduction-band states. A theoretical polaron mobility expression due to Langreth⁹ gives a room-temperature mobility of about 45 cm²/V sec using KM's values of mass and coupling constant, and about 2 cm²/V sec using the values of EPB. The experimental mobility value is about 15 cm²/V sec.^{5,7} Since the theoretical expression, by neglecting some scattering mechanisms, probably overestimates the mobility, it seems that EPB's values are not characteristic of polarons in the conduction band. The values determined by KM are therefore used in discussing the present work. The same transport studies have shown that the thermal ionization energy of the Y donor in lightly doped samples is less than 0.1 eV. At low temperature, impurity-band conduction is evident at all concentrations studied.¹⁰

With respect to optical properties, it is clear that there will be substantial polaron effects which influence the spatial distribution of the bound electrons and their ionization energies, and hence the observed optical absorption. The measurements cannot be extended to high temperature (>500°C) because the crystal reverts to the insulating state when heated to near the original Cd anneal temperature. In practice, this means that one cannot measure the optical absorption in the range where most of the carriers are free. The spectral range of the data is limited by the strong reststrahl edge of CdF₂ in the neighborhood of 0.07 eV. As we shall see, the induced infrared absorption overlaps this reststrahl band.

⁸ P. Eisenberger, P. S. Pershan, and D. R. Bosomworth, *Phys. Rev. Letters* **21**, 543 (1968).

⁹ D. C. Langreth, *Phys. Rev.* **159**, 717 (1967).

¹⁰ R. P. Khosla, D. Matz, and F. Moser, *Bull. Am. Phys. Soc.* **13**, 454 (1968).

¹ J. D. Kingsley and J. S. Prener, *Phys. Rev. Letters* **8**, 315 (1962).

² P. F. Weller, *Inorg. Chem.* **4**, 1545 (1965).

³ P. Eisenberger and P. S. Pershan, *Phys. Rev.* **167**, 292 (1968).

⁴ F. Trautweiler, F. Moser, and R. P. Khosla, *J. Phys. Chem. Solids* **29**, 1869 (1968).

⁵ J. S. Prener and H. H. Woodbury, in *Proceedings of the Seventh International Conference on the Physics of Semiconductors, Paris, 1964*, edited by M. Hulin (Academic Press Inc., New York, 1964), p. 1231.

⁶ D. R. Bosomworth, *Phys. Rev.* **157**, 709 (1967).

⁷ R. P. Khosla and D. Matz, *Solid State Commun.* (to be published).

II. EXPERIMENTAL DETAILS

The procedures used in growing the CdF_2 crystals have been described elsewhere.⁴ After growth, the crystals were annealed in Cd metal vapor at 500°C and cooled to room temperature over a period of about 1h to produce the semiconducting state. For the absorption studies, $\sim 2 \times 10$ -mm rectangular plates from 0.02 to 2 mm thick were cut and polished. Samples thinner than 0.02 mm were too fragile to handle. Since we studied the optical properties in transmission, this limited us to absorption coefficients below about 1500 cm^{-1} .

The spectral region from 0.2 to 3μ was covered by using a Cary model 14RI spectrophotometer in the forward mode. The region of 2 to 20μ was investigated with a Beckman IR 8 or Perkin Elmer 521 spectrophotometer. Absorption coefficients were determined after correcting the density for the loss due to reflection and scatter. Where possible, data from similar samples of different thicknesses were used to check absorption-coefficient values. We attribute the slight variations among samples to variations in electron concentration along a grown ingot. In some cases a small, spectrally neutral absorption was present, but this was not included in evaluating absorption coefficients.

The Y concentrations are nominal values added to the melt prior to growth. However, analytical checks on crystals by atomic absorption spectroscopy show good agreement between actual and nominal values.

III. EXPERIMENTAL RESULTS

The infrared absorption band induced by Cd anneal of Y-containing CdF_2 crystals is shown in Fig. 1. The nominal value of Y is $5 \times 10^{17}/\text{cm}^3$ and the measurement

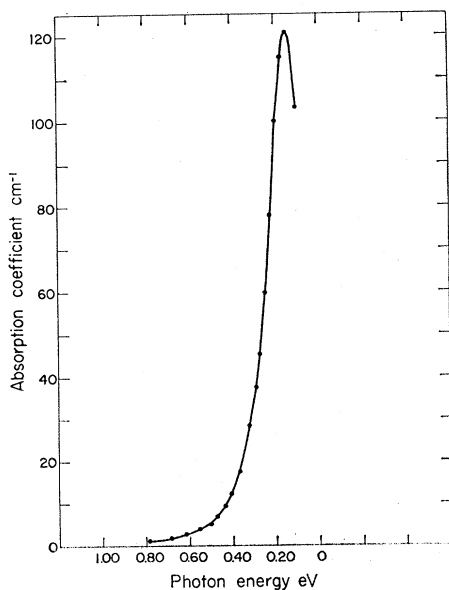


FIG. 1. Infrared absorption at 300°K in semiconducting $\text{CdF}_2:\text{Y}$ crystal containing a nominal addition of $5 \times 10^{17} \text{ Y/cm}^3$.

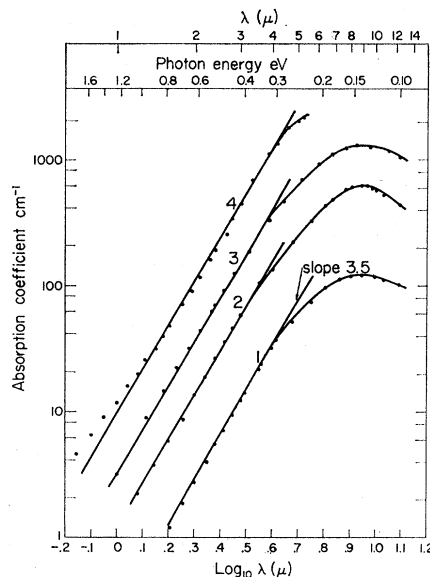


FIG. 2. Infrared absorption in semiconducting $\text{CdF}_2:\text{Y}$ crystals: at 300°K, at different Y concentrations. Curve 1: $0.5 \times 10^{18} \text{ Y/cm}^3$; curve 2: $1.3 \times 10^{18} \text{ Y/cm}^3$; curve 3: $2.6 \times 10^{18} \text{ Y/cm}^3$; curve 4: $2.6 \times 10^{19} \text{ Y/cm}^3$. The data are presented on a $\log_{10} \alpha$ versus $\log_{10} \lambda$ plot. A wavelength scale and an energy scale are shown for reference.

was made at room temperature. The band has a broad maximum in the neighborhood of 0.14 eV and a high-energy tail which extends to energies many times the peak energy value. The induced absorption for energies below about 0.1 eV cannot be measured because of the strong reststrahl absorption edge which begins just below this energy. The actual intensity of the band depends on the Cd treatment and on the Y concentration. The Cd treatment is sufficient to replace nearly all the compensating interstitial fluoride ions by electrons. Thus, one would expect the infrared-band intensity to be proportional to the Y concentration if no other compensating acceptors play a role. The infrared band as a function of Y concentration is shown in Fig. 2. The spectra are presented on a log absorption coefficient versus log wavelength scale to illustrate several features. First, the band intensity is proportional to the Y concentration for the two intermediate concentrations, but falls off for both the low and the high Y concentration. It seems likely that at low Y concentration ($5 \times 10^{17}/\text{cm}^3$), other compensating impurities play a role. A possible reason for the relatively weaker absorption at high Y concentration ($2.6 \times 10^{19}/\text{cm}^3$) will be considered in Sec. IV E. However, the band shape and peak position are relatively independent of concentration. Further, this plot reveals that for absorption coefficients below about 25% of the maximum, the high-energy tail has the functional form $\alpha = a\lambda^{3.5}$, except for the highest concentration sample. The deviation in that sample may be due to an uncertainty in the correction for a weak background absorption.

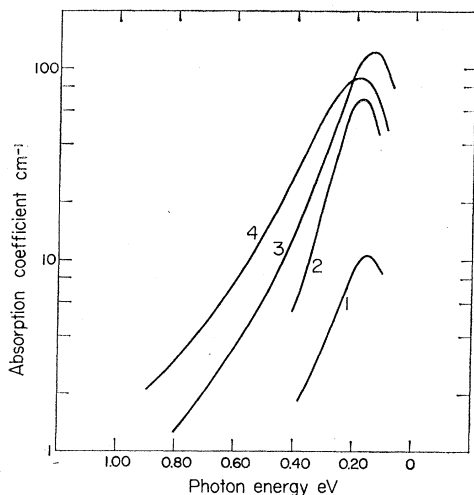


FIG. 3. Infrared absorption band in semiconducting CdF_2 with different donor impurities. In this case, the impurity concentrations are quoted as mole fractions and the temperatures are those at which the spectra were recorded. Curve 1: Eu, $1:10^3$, 350°K ; curve 2: Nd, $1:10^4$, 77°K ; curve 3: Y, $5:10^5$, 300°K ; curve 4: In, $1:10^3$, 300°K .

Similar but not identical infrared spectra have been observed in other semiconducting CdF_2 crystals. For example, Fig. 3 shows the infrared band for samples doped with Eu, Nd, Y, and In. Except for Nd,³ the samples were grown in our laboratory. Although the spectra were obtained at different temperatures and different dopant concentrations, the general features are similar. The peak varies by only a few hundredths of an electron volt, and a high-energy tail is present in all cases. This suggests that it is the excess positive

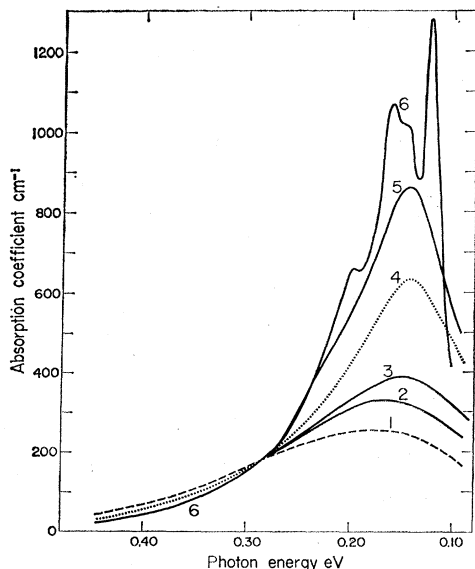


FIG. 4. Infrared absorption band in semiconducting $\text{CdF}_2:\text{Y}$ at various temperatures. The Y concentration is $1.3 \times 10^{18}/\text{cm}^3$. Curve 1: 520°K ; curve 2: 420°K ; curve 3: 370°K ; curve 4: 300°K ; curve 5: 175°K ; curve 6: 77°K .

charge of the center that determines the infrared absorption rather than the detailed atomic configuration of the particular impurity.

Only in the intermediate Y concentration samples has it been possible to obtain fairly complete spectra over a broad range of temperature. The spectra at temperatures between 77 and 520°K are shown in Fig. 4 for a sample containing $1.3 \times 10^{18} \text{ Y}/\text{cm}^3$. Similar results were obtained on the $2.6 \times 10^{18} \text{ Y}/\text{cm}^3$ sample. As the temperature is lowered, the peak near 0.15 eV becomes more intense. At the lowest temperature investigated, considerable structure begins to appear with well-defined peaks at about 0.20 , 0.16 , and 0.12 eV .¹¹ The high-energy tail decreases in intensity with decreasing temperature. These features will be discussed in some

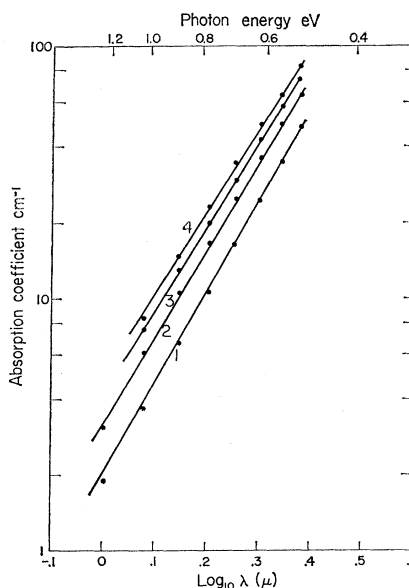


FIG. 5. High-energy infrared absorption tail in semiconducting $\text{CdF}_2:\text{Y}$ at various temperatures. The Y concentration is $2.6 \times 10^{18}/\text{cm}^3$. Curves 1-4 are at 80 , 300 , 380 , and 450°K , respectively. The straight lines have slope 3.5 , 3.5 , 3.3 , and 3.2 , respectively.

detail in the next section, but it is of interest that the high-energy tail retains nearly the same functional form over this temperature range. This is illustrated in Fig. 5, where the high-energy tail is shown, again on a log-log plot, for a $2.6 \times 10^{18}/\text{cm}^3$ doped sample. The $\lambda^{3.5}$ dependence observed at room temperature is retained at the low temperature. At higher temperature the dependence is weaker, approximating a $\lambda^{3.2}$ power law.

IV. DISCUSSION

A. Origin of Infrared Band

At low temperature, where most of the Y donors are not ionized, the observed infrared band must arise from

¹¹ Recently, T. H. Lee, of our laboratory, has extended these studies to 4.2°K , has confirmed this structure, and has revealed some additional structure in the spectrum.

transitions between bound states of the un-ionized donor or transitions from such states to the conduction band. At high temperature, there is a contribution from intraband transitions of free carriers. We have examined the data for correlations between the absorption band and the concentration of both free carriers (n) and un-ionized donors (N_{un}). The carrier concentration n at temperatures up to 420°K has been determined by Hall coefficient measurements in the same sample for which spectral data are available. The number of un-ionized donors is given by $N_{\text{un}} = (N_D - N_A) - n$, where N_D is the total concentration of donors and N_A the acceptor concentration. N_D is equal to the total Y concentration. We have no direct measure of N_A , but we estimate that it is less than $2 \times 10^{17}/\text{cm}^3$ in this sample. This estimate follows from the fact that the Hall coefficient shows no clear evidence of an exhaustion region up to the highest temperature measured, and that the high-energy infrared absorption tail increases in intensity up to at least 520°K . Table I gives the carrier concentration and un-ionized donor concentration at various temperatures, and the intensity of the infrared band near the peak and in the high-energy tail. The data show correlations which are illustrated in Fig. 6. In this figure, the free carrier concentration, the number of un-ionized donors, and the absorption coefficients near the peak (0.15 eV) and in the high-energy tail (0.8 eV) are all plotted as a function of reciprocal temperature. It is clear that the peak absorption correlates with the number of un-ionized donors. The tail absorption also shows a correlation with free carrier concentration at high temperature ($10^3/T < 3$). At lower temperature, the tail absorption correlates neither with the free carrier concentration nor with the total number of un-ionized donors. However, we believe that the tail absorption, and hence the $\lambda^{3.5}$ spectral dependence, is attributable primarily to transitions from isolated donors. (This is discussed in Sec. IV E.) At high temperature, when free carrier contributions in the tail become appreciable, the dependence on wavelength is weaker, as seen in Fig. 5. This indicates that the free carrier absorption has a spectral dependence which goes as a lower power of the wavelength. One cannot carry out a more quantitative decomposition of the observed absorption, since there is no independent measure of how the two contributions

TABLE I. Relation between carrier concentrations and infrared absorption in $\text{CdF}_2:\text{Y}$, with Y concentration $1.3 \times 10^{18}/\text{cm}^3$.

Temp. ($^\circ\text{K}$)	$10^3/T$ ($^\circ\text{K}^{-1}$)	Carrier conc. n ($10^{17}/\text{cm}^3$)	Un-ionized donor concn- tration N_{un} ($10^{17}/\text{cm}^3$)	Absorption strength α (cm^{-1})	
				at 0.15 eV	at 0.80 eV
175	5.7	1.1	11.9	840	5.2
300	3.3	4.4	8.6	620	6.7
370	2.7	5.9	7.1	375	8.7
420	2.4	6.9	6.1	325	9.7
470	2.1	7.8	5.2	290	11.5

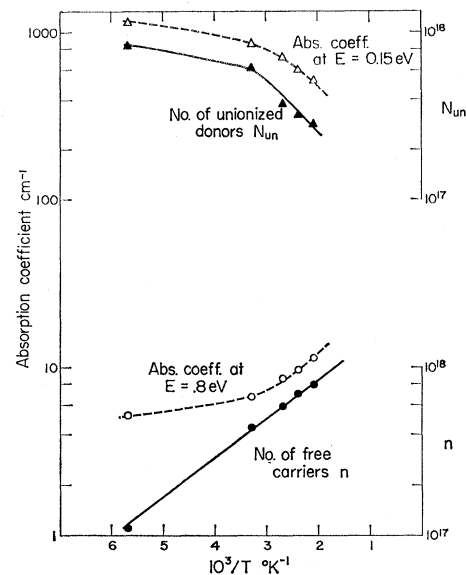


Fig. 6. Carrier concentration (n), un-ionized donor concentration (N_{un}), and the absorption coefficient in the high-energy tail ($E=0.80$ eV) and near the peak ($E=0.15$ eV) all plotted as a function of reciprocal temperature.

change shape with changing temperature. The subsequent discussion will deal primarily with the nature of the ground state of the Y donor in CdF_2 . If we neglect donor interaction effects, which give rise to an impurity bound to a center we wish to consider is an electron bound to an excess positively charged substitutional ion (Y^{3+}) in an ionic solid. The fact that the infrared absorption band is similar for different dopants suggests that it is primarily the excess charge of the center which determines the potential in which the electron moves. The bound electronic states of such a system have been treated theoretically in a continuum model in the limits of the nonadiabatic approximation by Buimistrov,¹² and in an adiabatic approximation by Kubo¹³ and by Simpson.¹⁴ Platzman¹⁵ has calculated the ground state of the bound polaron in a form valid for all electron-phonon coupling constants, and all electron impurity binding energies. However, the form of his results, particularly for the intermediate case, requires lengthy and difficult computations to obtain numerical values of the binding energy. For a preliminary qualitative understanding of the donor states of Y in CdF_2 , such computations are not necessary. In the adiabatic limit, the evaluation of Platzman's formula is more easily carried out in the framework of a recent paper by Perlin and Gifeisman.¹⁶

¹² V. M. Buimistrov, *Fiz. Tverd. Tela* **5**, 3264 (1963) [English transl.: *Soviet Phys.—Solid State* **5**, 2387 (1964)].

¹³ R. Kubo, *J. Phys. Soc. Japan* **3**, 254 (1948).

¹⁴ J. H. Simpson, *Proc. Roy. Soc. (London)* **A231**, 308 (1955).

¹⁵ P. M. Platzman, *Phys. Rev.* **125**, 1961 (1962).

¹⁶ Yu. E. Perlin and Sh. N. Gifeisman, *Fiz. Tverd. Tela* **9**, 2752 (1967) [English transl.: *Soviet Phys.—Solid State* **9**, 2165 (1968)].

TABLE II. Optical constants and carrier masses in CdF₂.

Temp. (°K)	(a) Optical constants ^a			
	ϵ_∞	ϵ_0	TO (cm ⁻¹)	LO (cm ⁻¹)
300	2.40	8.49	202	380
80	2.40	7.78	224	403

(b) Carrier masses^b

Polaron mass $m_p \cong 0.9m_e$
 Conduction-band mass $m_c \cong 0.45m_e$
 Coupling constant $\alpha \cong 3.3$

^a Reference 6.^b Reference 7.^c m_e is the free-electron mass.

Using this work, we have calculated the binding energy for CdF₂ in the nonadiabatic limit, and found agreement with the Buimistrov theory. We will therefore refer to Buimistrov's work when considering the nonadiabatic limit.

We attach the usual meaning to the terms "adiabatic" and "nonadiabatic" limit. In the former case the lattice cannot follow the instantaneous position of the electron, responding only to some average electron charge distribution; in the latter case the lattice can more or less follow the instantaneous electron position. A quantitative measure of the range of validity of the approximations is obtained by comparing the average electron kinetic energy

$$\hbar^2/2m_e r_0^2$$

to the optical phonon energy ($k\theta$), where r_0 is a measure of the mean electron charge distribution. The adiabatic approximation is valid for $\hbar^2/2m_e r_0^2 \gg k\theta$, and the nonadiabatic approximation applies if $\hbar^2/2m_e r_0^2 \lesssim k\theta$.

In the next sections we examine the question of which approximation, if any, provides a self-consistent description of the states of isolated Y donors in CdF₂. The dielectric constant, carrier masses, and phonon energies that enter as parameters in the discussion are given in Table II. The importance of donor interactions in interpreting the results of optical and transport studies is discussed in Sec. IV E.

B. Nonadiabatic Approximation

The simplest model would consider the Y³⁺ electron as a hydrogenlike donor with the electron in a large-orbit 1s ground state. The optical or thermal ionization energy E_i and the effective Bohr radius r_0 of the ground state are given by $E_i = E_R m^*/\epsilon^2$ and $r_0 = a_0 \epsilon/m^*$, where $E_R = 13.1$ eV, $a_0 = 0.52$ Å, and m^* and ϵ are an appropriate electron mass and dielectric constant, respectively. If the ground-state orbit is moderately large, the situation can be viewed as a polaron moving in a medium of dielectric constant ϵ_0 . Using the values given in Table II, one obtains $E_i \cong 0.18$ eV and $r_0 \cong 5$ Å. The absorption spectrum shows major peaks at about 0.20, 0.16, and 0.12 eV. We assume that one of these peaks, probably the high-energy one, corresponds to the optical energy required to ionize the donor, and that the lower-energy

peaks arise from transitions to lower excited states. If this identification is correct, there is reasonable agreement between the calculated ionization energy and the observed optical energy. There is large disagreement, however, with the ionization energy of about 0.1 eV determined from transport studies, and we shall comment on this in Sec. IV E. The calculated Bohr radius of 5 Å implies a kinetic energy $\hbar^2/2m_e r_0^2$ of about three times the optical phonon energy of 0.05 eV. At this relative energy, the nonadiabatic limit cannot be completely valid. A more rigorous theoretical treatment of the hydrogenlike center in a polarizable medium has been given by Buimistrov.¹² The Buimistrov theory has been applied to the silver halides by Brandt¹⁷ and he has derived explicit expressions for the thermal ionization energy and Bohr radius. These differ from the simpler hydrogenic model considered in the preceding paragraphs. If one applies the expressions derived by Brandt to CdF₂, using $m_c = 0.46m_e$ and $m_p = 0.92m_e$, one obtains values of 0.15 eV for the ionization energy and 6.5 Å for the ground-state Bohr radius. Again, the energy is in the vicinity of the optical absorption peak. The slightly larger Bohr radius is an improvement, but still gives a kinetic energy larger than the optical phonon energy. While not completely consistent with the nonadiabatic approximation, such relative energies would still allow the lattice to respond to the instantaneous electron position to a large extent. This model, however, does not allow for large differences in optical and thermal ionization energies.

C. Adiabatic Approximation

The other extreme is to regard the electron as being in a fairly compact ground state, assume that the adiabatic approximation is valid, and view the electron as a particle with a conduction-band mass moving in a screened impurity potential $-e/\epsilon^*(r)$. Here, $\epsilon^*(r)$ is a self-consistently determined dielectric constant, and will involve some sort of average between the static and high-frequency constants. Kubo¹³ and Simpson¹⁴ have given independent theoretical treatments of the states of an electron bound to a positive charge center in an ionic solid in this adiabatic limit. Their results are essentially identical. They obtain explicit expressions for the optical (E_{op}) and thermal (E_{th}) ionization energies. These are

$$E_{op} = \frac{e^4 m_c}{2\hbar^2} \left(\frac{1}{\epsilon_0} + \frac{5}{16} C \right) \left(\frac{1}{\epsilon_0} + \frac{15}{16} C \right),$$

$$E_{th} = \frac{e^4 m_c}{2\hbar^2} \left(\frac{1}{\epsilon_0} + \frac{5}{16} C \right)^2,$$

where $C = 1/\epsilon_\infty - 1/\epsilon_0$. The other quantities have their

¹⁷ R. C. Brandt, Ph.D. thesis, University of Illinois, 1967 (unpublished).

usual meaning. The effective Bohr radius is given by

$$r_0 = \frac{a_0}{m_c \epsilon_0} \left(\frac{1}{16} + C \right)^{-1}.$$

If those expressions are applied to CdF₂, using $m_c = 0.46m_e$, $\epsilon_0 = 7.8$, and $\epsilon_\infty = 2.4$, one obtains $E_{op} = 0.54$ eV, $E_{th} = 0.23$ eV, and $r_0 = 5.3$ Å. The average electron kinetic energy $\hbar^2/2m_c r_0^2$ is about $5k\theta$. Although the ratio of calculated optical to thermal energies is about that observed experimentally (assuming $E_{th} \sim 0.1$ eV from Hall data and $E_{op} \sim 0.2$ eV), their magnitude is much too large. Further, the adiabatic approximation is valid only if the kinetic energy is very large compared to the optical phonon energy. At $\hbar^2/2m_c r_0^2$ about $5k\theta$, the lattice still can respond to a considerable extent to the instantaneous electron position. The poor agreement of calculated and observed ionization energies and the lack of self-consistency mean that the adiabatic approximation is not an adequate description of this center.

D. Photo-Ionization Processes

The discussion up to this point has been concerned with the peak absorption in the optical spectrum. The other prominent and reproducible feature of the infrared band is the functional form of the high-energy tail. Over a broad range of concentration, and for temperatures at which free carrier absorption is negligible, the absorption coefficient varies as the 3.5th power of the wavelength.

It seems likely that the observed functional form is a consequence of a photo-ionization process. The photo-ionization spectrum of a hydrogen atom has been treated theoretically by Hall.¹⁸ Fan¹⁹ has pointed out that the Hall expression can be taken over to the case of a hydrogenic donor in a solid if one neglects the periodic variation of the electron wave function in a crystal, and simply uses the effective-mass formalism and a Coulomb wave function as the final electron state. For energies E large compared to the ionization energy E_i , Fan shows that the absorption coefficient $\alpha(E)$ is given by

$$\alpha(E) = \frac{5.26 \times 10^{-17}}{n} N \frac{m_e E_R}{m_c E_i} \left(\frac{E_i}{E} \right)^{3.5},$$

where N is the total number of centers, n is the refractive index, and E_R the rydberg unit of energy. This expression obviously gives the $\lambda^{3.5}$ ($\equiv 1/E^{3.5}$) dependence experimentally observed in the high-energy tail. From curve 1 of Fig. 5, the experimental value of α at low temperature at $E = 1.0$ eV is about 4 cm^{-1} . The number of donors in this sample is $2.6 \times 10^{18}/\text{cm}^3$, and at this temperature essentially none of the donors is ionized. Using these values, and assuming $m_c \cong 0.46m_e$ and

$E_i \sim 0.20$ eV, the theoretical expression for α gives a value of about 40 cm^{-1} . Even for $E_i \sim 0.15$ eV, the calculated value is still about 20 cm^{-1} . Thus, the experimental value is only about $\frac{1}{10}$ the calculated value. This could be explained if compensating impurities were present in a concentration nearly equal to the donor concentration. However, we estimate the acceptor concentration as being, at most, a few tenths of the donor concentration in this sample (see Sec. IV A). It appears that only a small fraction of the donors contribute to the absorption in the high-energy tail. A possible interpretation of this observation is discussed in Sec. IV E.

A different approach to calculating the photo-ionization spectrum of a shallow donor state has been taken by Kukimoto *et al.*²⁰ Assuming a simple parabolic conduction band, they calculate exact energy-momentum relationships and electron wave functions in the neighborhood of $k=0$, using the $k \cdot p$ perturbation method. The treatment also allows for the possibility of different optical and thermal ionization energies, but does not apparently take into account the modification of the wave functions in the vicinity of the impurity. Kukimoto *et al.* obtain the expression

$$\alpha(E) = \alpha_0 \frac{(E - E_{op})^{3/2}}{E(E - E_{op} + E_{th})^4},$$

with

$$\alpha_0 = \frac{32\sqrt{2}\pi e^2 \hbar^6 N_D}{nc(m_c)^{7/2} r_0^5}.$$

All the parameters have been defined previously. For energies large compared to E_{op} and E_{th} , this expression also gives a spectral dependence of the form $\lambda^{3.5}$. The magnitude is extremely sensitive to the choice of r_0 . Using $m_c = 0.46m_e$, there is numerical agreement with the Hall formula at $E = 1.0$ eV for r_0 approximately 9 Å. The value of $r_0 = 5.3$ Å obtained by applying Simpson's expression, which should apply to the work of Kukimoto *et al.*, gives a calculated α about two orders of magnitude larger than the experimental value. A similar difficulty has been noted by Kukimoto *et al.*²⁰ for Al donors in ZnS.

It is interesting to note that both forms of the photo-ionization cross sections discussed give the $\lambda^{3.5}$ spectral dependence because the ground-state wave function is assumed to be of a hydrogenic $1s$ character. Thus, the observed $\lambda^{3.5}$ spectral shape in CdF₂ suggests that the ground-state electron wave function is indeed close to being a hydrogenic $1s$ -like state.

E. Conclusions

In summarizing our results, we are faced with the following difficulties. Within the continuum model of the electron-phonon interaction, the thermal ionization

¹⁸ H. Hall, Rev. Mod. Phys. **8**, 359 (1936).

¹⁹ H. Y. Fan, Rept. Progr. Phys. **19**, 107 (1956).

²⁰ H. Kukimoto, S. Shionoya, T. Koda, and R. Hioki, J. Phys. Chem. Solids **29**, 935 (1968).

energy must lie between the value of 0.15 eV predicted in the nonadiabatic limit and 0.23 eV predicted in the adiabatic limit. The optical ionization energy must be at least this large. In fact, the optical ionization energy observed experimentally is in this range, but the thermal ionization energy, determined from resistivity and Hall coefficient measurements, does not exceed 0.1 eV. The transport measurements also show that impurity banding is important even in the lowest concentration samples, and increases with increasing concentration at low temperature.¹⁰ The optical absorption band does not change shape, however, over the whole concentration range studied, from about 5×10^{17} to $2 \times 10^{19}/\text{cm}^3$. Further, the optical band shows features which seem to rule out the possibility that the absorption band arises from transitions originating from an impurity-band ground state. In particular, the well-resolved structure and the high-energy $\lambda^{3.5}$ photo-ionization tail are inconsistent with such a ground state. The $\lambda^{3.5}$ spectral shape is indicative of photoionization from isolated approximately hydrogenlike donors. Photo-ionization from a delocalized impurity-band ground state would give rise to a steeper photoionization tail.

This lack of a clear correlation between the optical and transport properties seems superficially to raise difficulties in understanding, but in fact suggests a possible interpretation of the results. We assume that the donor impurities in CdF_2 are not randomly distributed, but have a tendency to form clusters. Evidence for such a nonrandom distribution of donors has recently been provided by the work of Eisenberger and Pershan.³ Such clusters would give regions of locally high donor concentration, and a proportionally small fraction of isolated impurities for which interaction effects may be neglected.

We view the low-temperature optical absorption as arising primarily from the small fraction of such isolated donors, while the impurities in clusters give rise to impurity-banding effects and are responsible for the observed transport behavior. Interaction effects of electrons in these clusters effectively reduce their binding energy and lead to the observed thermal ionization energy of 0.1 eV. Optical transitions from this impurity band, which may be of variable width throughout the crystal, would contribute a background absorption. Since the isolated donors are assumed to be small in number at all concentrations, the optical absorption as-

sociated with them would be small compared to the intensity predicted by assuming that all the donors are isolated. This is consistent with the discussion of the photoionization transitions in Sec. IV D. It is also consistent with the observation that the intensity of the high-energy absorption tail does not correlate with the total number of un-ionized donors at low temperature.

If this general picture is correct, a model for the isolated center need not necessarily predict different optical and thermal ionization energies. In view of this, the continuum model based on the nonadiabatic approximation becomes a more tenable model. The ionization energy it predicts is consistent with the observed optical spectra, and the ground-state kinetic energy is still small enough to allow for dynamic polarization effects. Thus, the picture of isolated donors described by a continuum theory in the nonadiabatic limit, and the presence of impurity clusters, provides a framework within which we can get a qualitative understanding of the optical and transport behavior. The optical energies predicted by a continuum adiabatic model are inconsistent with the observed spectra and carrier mass. However, neither of the continuum models is entirely satisfactory, and it is possible that a noncontinuum description may ultimately yield a more satisfactory model. In any case, transport and optical measurements on much more lightly doped samples, in which impurity banding would be small, are needed to confirm the existence of the postulated larger thermal activation energy for isolated donors. At present, the best crystals are not sufficiently pure to allow doping at concentrations below about $5 \times 10^{17}/\text{cm}^3$.

ACKNOWLEDGMENTS

Professor F. Brown, at the University of Illinois, contributed to this work by discussions and by making available computer calculations of the energies based on the Buimistrov theory. Our interest in this system was stimulated by many discussions with F. Trautweiler, as well as with R. P. Khosla, who also made available the results of his transport studies of this material. T. H. Lee and L. Costa made available their infrared instrumentation and experience. R. Gluck and W. Pinch prepared the samples used in these studies. R. Ambrose provided analytical determinations of the Y content in these samples. To all of these people we express our thanks for their contribution to the work.